*Materials Science and Engineering*, 59 (1983) 235–249





# The Attenuation of Shock Waves in Nickel: Second Report

MARC A. MEYERS, KOU-CHANG HSU and KAREN COUCH-ROBINO

*Department of Metallurgical and Materials Engineering, New Mexico Institute of Mining and Technology, Socorro, NM 87801 (U.S.A.)*

(Received September 16, 1982; in revised form November 15, 1982)

SUMMARY

*Continuation of the investigation whose initial results were reported earlier revealed that the decrease in the tensile properties of shock-loaded nickel as a function of distance from the impact surface was consistent with the decrease in hardness and dislocation density, as well as the decay of the shock pulse.*

*On uniaxial tensile testing of the specimens subjected to a 25 GPa pulse and in the pre-shocked condition, work softening was clearly observed. Work softening was eliminated by an appropriate anneal that stabilized the substructure without significantly affecting the yield stress. Transmission electron microscopy of the work-softened region revealed that the shock-induced substructure was replaced by elongated cells with well-defined walls having a high dislocation density.*

## 1. INTRODUCTION

Hsu *et al.* [1] have recently described the effects of microstructural parameters on the attenuation of shock waves in nickel. The most important conclusion of their investigation is that the grain size and dislocation substructure have no noticeable effect on the rate of decay of the pressure pulse. These results are in good agreement with an investigation conducted on Fe–15wt.%Cr–15wt.%Ni and Fe–34.5wt.%Ni monocrystals and polycrystals; the polycrystallinity did not seem to affect the shock pulse propagation [2]. It was also found [2] that the polycrystals exhibited a lower hardness increase than the monocrystals and bicrystals. The attenuation of shock waves in solids has received some attention in the past, starting with the early considerations of Rayleigh [3] and Taylor [4]. However, it was the introduction of an "artificial viscosity" term by von Neumann and Richtmyer [5] that allowed a direct consideration of the internal dissipative processes. Erkman [6], Drummond [7], Fowles [8], Erkman and coworkers [9–11] and Curran [12] investigated the attenuation of shock waves; the consensus is that the observed rate of attenuation is much higher than that predicted from the hydrodynamic theory. Although these investigators proposed models predicting higher attenuation rates, they did not present a physical description of the internal processes responsible for attenuation; an attempt to do this was made by Hsu *et al.* [1] who proposed an accumulation model. According to their model, the heat generated by dislocation motion during the passage of the shock wave is the main energy dissipation mechanism. While Hsu *et al.* [1] concentrated on the micromechanical processes responsible for the attenuation of the shock pulse and on the resultant dislocation substructures, the investigation whose results are reported herein focused primarily on the tensile properties of nickel in the *post explosionem* condition. An interesting response of the shocked nickel, work softening, that had been observed earlier [13] was confirmed and investigated in greater detail. The term work softening designates the yielding drop behavior of a metal undergoing tensile testing, contrary to the normally encountered work hardening. A number of investigators have observed the phenomenon, which was systematically studied by Longo and Reed-Hill [14–16]. They obtained this behavior by prestraining f.c.c. polycrystalline metals of moderate to high stacking fault energy at a low temperature (77 K) and continuing the tensile deformation at higher temperatures. During the higher temperature part of the deformation the dislocations

generated at the lower temperatures were able to cross slip and climb with the help of thermal activation, with the result that the substructure generated at the low temperature was replaced by the substructure stable under the imposed conditions (the higher temperature portion of deformation). The same rationale was applied by Meyers [13] to explain work softening in shock-loaded nickel.

## 2. EXPERIMENTAL TECHNIQUES

The experimental system used to produce the shock waves and to monitor their attenuation has been described previously by Hsu *et al.* [1]. Two nominal initial pressures were used: 10 and 25 GPa. The initial nominal pulse duration was 2 $\mu$s. For the lower pressure experiments an inclined-plate system was used; for the 25 GPa experiments a parallel plate with a plane wave generator was used. Both set-ups are shown in Fig. 1, which depicts schematically the experimental arrangement and the position of the manganin piezoresistive gauges. Three metallurgical conditions were used at each pressure: two annealed conditions (with grain sizes of 32 and 150 $\mu$m) and one deformed condition (with a dislocation density of $2.7 \times 10^{10}$ cm$^{-2}$) obtained by preshocking the annealed large-grain-size nickel plates to a peak pressure of 14.2 GPa by contact explosives. Consequently, the total number of actual events was equal to six; in addition, two preliminary experiments using steel systems were conducted, to verify the circuiting and gauges.

The tensile tests were conducted on cylindrical specimens having a reduced gauge diameter of 4.8 mm ($\frac{3}{16}$ in) and a length of 44.5 mm ($1\frac{3}{4}$ in); an MTS universal testing machine (model 661.2) equipped with a 12.77 mm extensometer was used. The nominal initial strain rate was the same for all the tests: $5 \times 10^{-4}$ s$^{-1}$. The specimens that required annealing were inserted in stainless steel bags (Sen–Pak) to avoid oxidation. The shock-loaded specimens were machined from the shock-loaded plates in such a way that the tensile axis was perpendicular to the direction of propagation of the shock wave. The small-grain-size plates were rolled prior to the recrystallization treatment; for these conditions the tensile axis was chosen to be parallel to the rolling direction. The same orientation relationship was maintained for the specimen that was cold rolled to a reduction of 20%.

For the observation of the deformation zone around the hardness indentation, the

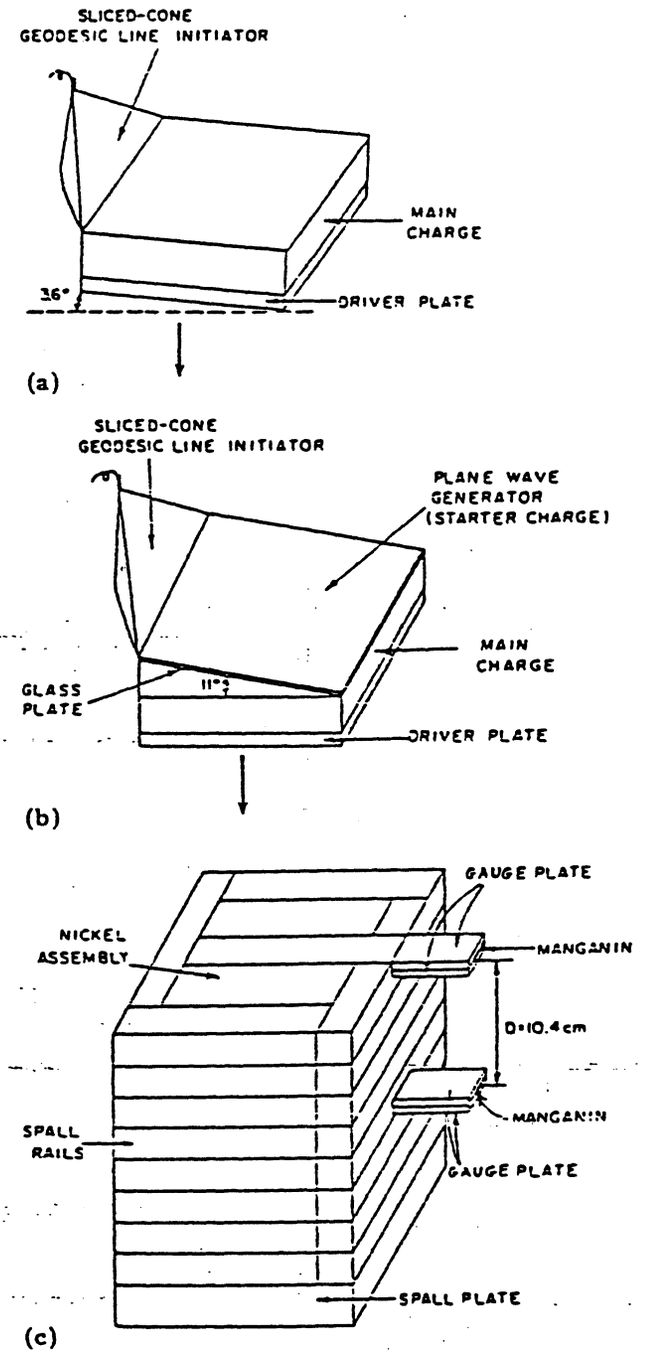


**Fig. 1. Experimental systems. Two flyer plate accelerators are shown: (a), (b) the inclined-plate accelerator was used for the 10 GPa events and (c) the parallel-plate accelerator was used for the 25 GPa events.**

surface of the specimens was electropolished and a steel ball (Rockwell B) 1.6 mm in diameter was used; loads of 60 and 100 kgf were used for the preshocked and post-shocked conditions respectively, resulting in indentations that had approximately the same diameter.

All experimental details or conditions not given here have been reported previously by Hsu *et al.* [1].

## 3. RESULTS AND DISCUSSION

### *3.1. Pressure gauge readings*

The manganin piezoresistive gauge outputs are shown in Fig. 2. Three gauges (shown by arrows) broke during the passage of the pulse. The details of the instrumentation nave been given by Hsu *et al.* [1] and in the theses of C. Y. Hsu [17] and K.-C. Hsu [18].

The steel events were used as a preparation for the nickel events. The distance between the gauges was smaller: 44.5 mm. In Fig. 2(a) the velocity of the shock pulse can be computed from the difference in the time $t$ of arrival between the pulses. It is found to be equal to 4.73 mm $\mu s^{-1}$, which compares reasonably well with the velocity reported in the literature [19]: 4.61 mm $\mu s^{-1}$. The same procedure was used for the nickel systems, and velocities of 4.5 mm $\mu s^{-1}$ and 4.65 mm $\mu s^{-1}$ were found for the 10 GPa events and 25 GPa events respectively; the velocities reported

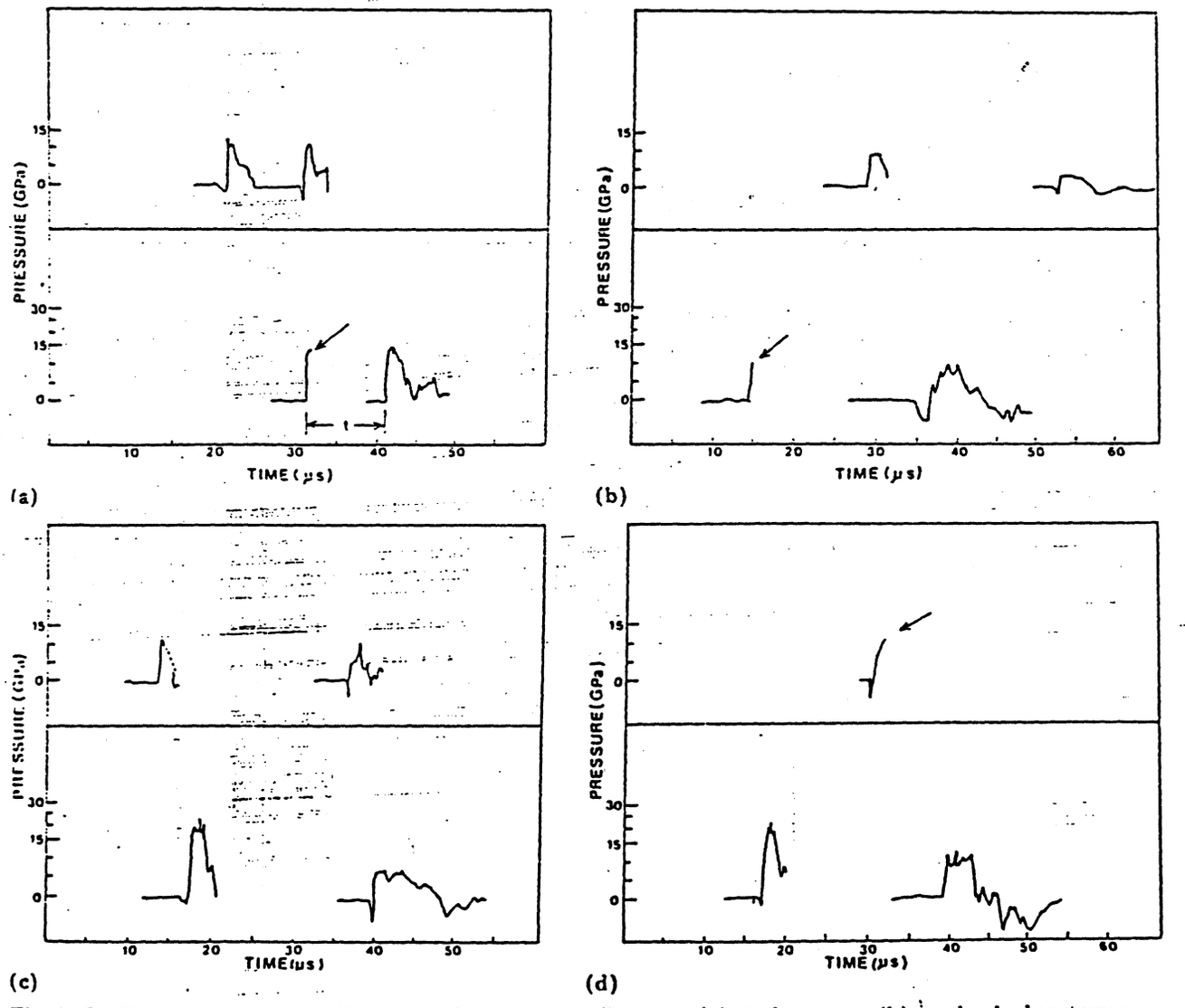


Fig. 2. Oscilloscope traces from the manganin gauges for all events: (a) steel systems; (b) preshocked systems; (c) large-grain-size (150 μm) systems; (d) small-grain-size (32 μm) systems: upper curves, 10 GPa events; lower curves, 25 GPa events.

[19] are 4.75 and 5.14 mm $\mu s^{-1}$; pressure changes were averaged in order to obtain the calculated velocities. A short tensile pulse was obtained prior to the arrival of the shock pulse in a number of the experiments; the reason for this pulse is not known. Monitoring of the shock pulse in explosively driven systems is very difficult, as evidenced by the irregularities in the shape of the pulses. However, a few important conclusions can be drawn.

(a) The shape of the pulse is much more irregular than that calculated. This could be due to the intrinsic pulse irregularities or to the gauge effects. Therefore, it becomes meaningless to discuss small changes in pulse duration, rarefaction rate or pressure; the irregularities would overshadow the differences. To obtain a well-characterized and "clean" pulse, the use of gas guns or an equivalent instrument is an absolute requirement.

(b) The attenuation rate is much higher than that predicted by hydrodynamic theory. Hsu *et al.* [1] present an "accumulation model" which takes into account the internal energy dissipation mechanisms (dislocation motion seems to be the main mechanism) responsible for the higher attenuation rates.

(c) The metallurgical condition (the grain size and dislocation substructure) seems to have no effect on the attenuation rate. This is clearer for the 25 GPa events, for which gauge outputs are available for the three conditions.

(d) The rate of release of the shock pulse is not linear; for the gauges close to the impact surface in the high pressure events of Figs. 2(c) and 2(d) an irregularity can clearly be seen in the rarefaction portion of the pulse.

(e) The calculated and measured pressures, pulse durations and rarefaction rates are in reasonable agreement.

### 3.2. *Hardness measurements*

The results of the hardness measurements are given here in separate plots, in Fig. 3 for the low pressure events and in Fig. 4 for the high pressure events. There is a considerable increase in hardness for both the small- and the large-grain-size events, even at the bottom of the system. In contrast, the preshocked strengthening effect occurred only to 8 cm from the impact surface for the 10 GPa events and to 15 cm from the impact surface for the 25 GPa events. From the oscilloscope gauges it can be seen that for the 25 GPa events the pressure is approximately 10 GPa at the

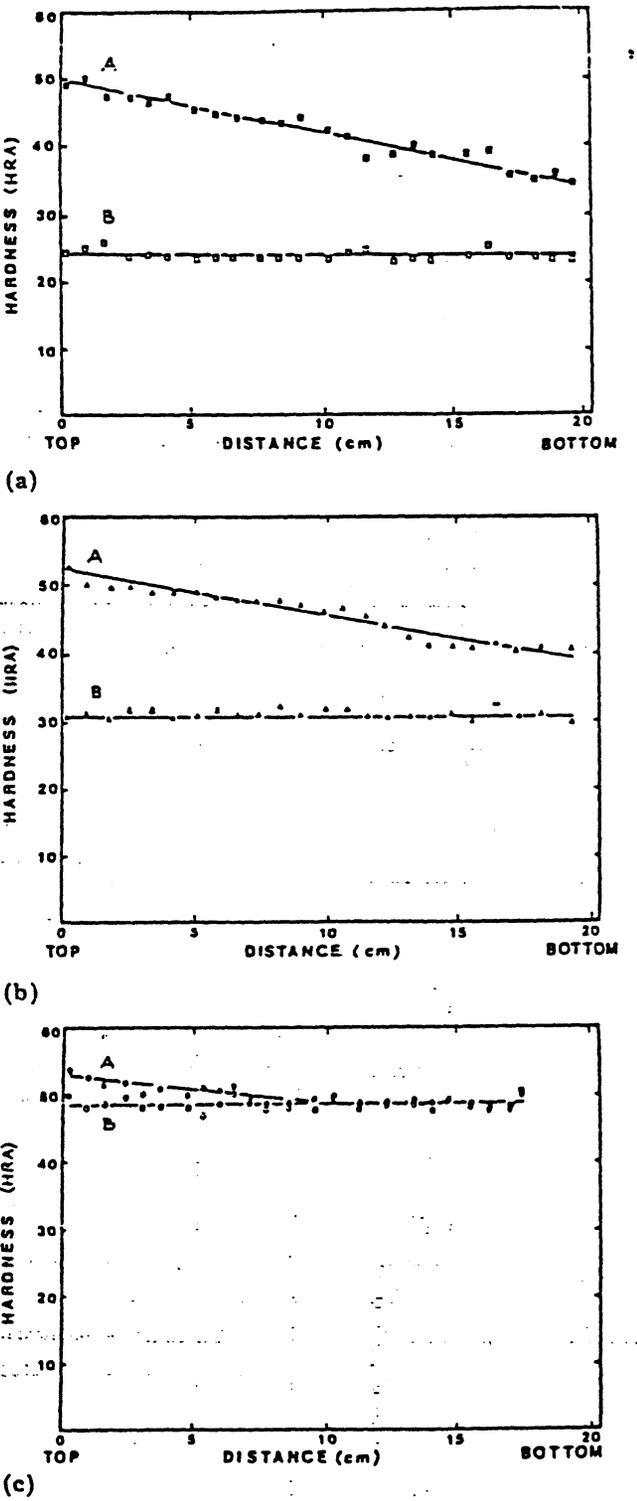


Fig. 3. Hardness profiles for all systems shocked at 10 GPa before shocking (lines B) and after shocking (lines A): (a) large-grain-size systems; (b) small-grain-size systems; (c) preshocked systems.

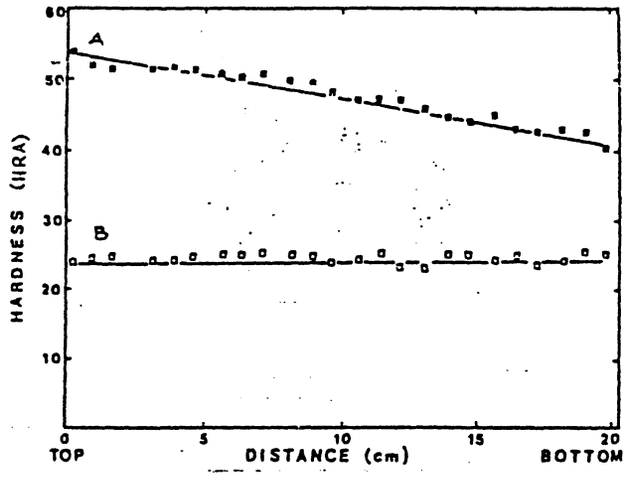


(a)

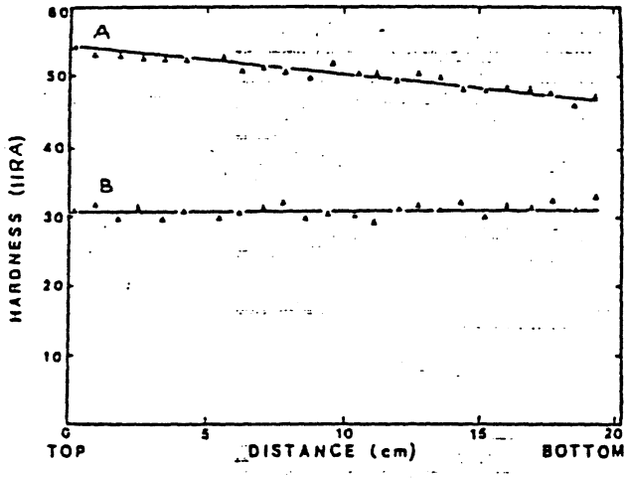


(b)

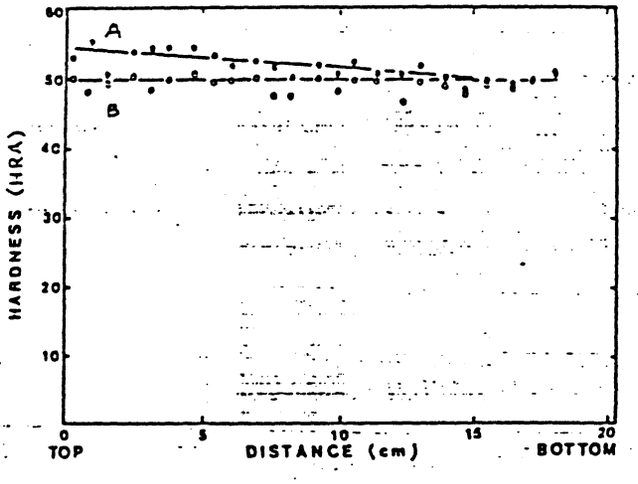


(c)

Fig. 4. Hardness profiles for all systems shocked at 25 GPa before shocking (lines B) and after shocking (lines A): (a) large-grain-size systems; (b) small-grain-size systems; (c) preshocked systems.

bottom gauge (about 11 cm from the impact interface). For the large- and small-grain-size systems the hardness readings at this position for the 25 GPa events (Figs. 4(a) and 4(b)) are very close to the initial hardnesses for the low pressure events (Figs. 3(a) and 3(b)); hence there is good agreement between the hardness and the gauge results.

From the linear decrease in hardness exhibited by the annealed conditions, the distance over which a shock wave will propagate (on the assumption of linearity) can be extrapolated from the intersection between the two lines in Figs. 3(a), 3(b), 4(a) and 4(b). A distance of 30 cm is found for the 10 GPa events; for the 25 GPa events a distance of 60 cm is obtained for the small-grain-size systems, and a distance of 45 cm for the large-grain-size systems.

In addition to the change in hardness, there were attendant changes in the shape of the deformation zone surrounding the indentation. It is worth commenting on these changes, since they are a manifestation of work softening. Figures 5(a) and 5(b) are photomicrographs of hardness indentations of annealed and shock-loaded (preshocked plus 25 GPa) specimens respectively. The pile-up of metal around the indentation is a well-known characteristic of work-hardened metals [20, 21]; in contrast, the deformation zone around an indentation in an annealed metal is much larger, and no pile-up is evident. The shocked specimen which exhibits work softening should show this effect to an even greater extent, and the slip band density is much higher (Fig. 5(b)). The same effect was observed by Meyers *et al.* [2] in shock-loaded Fe–34wt.%Ni alloy. A brief qualitative explanation is as follows. As the indenter penetrates into the specimen, the metal deforms. In the annealed condition it work hardens, so that additional deformation takes place in regions farther and farther away from the indentation. In the shock-loaded condition the deformed material work softens with an attendant decrease in the flow stress; hence, further deformation tends to concentrate and a bulge (a "pile-up") forms around the indentation.

### *3.3. Tensile response*

The change in tensile properties was studied by taking specimens (two for each

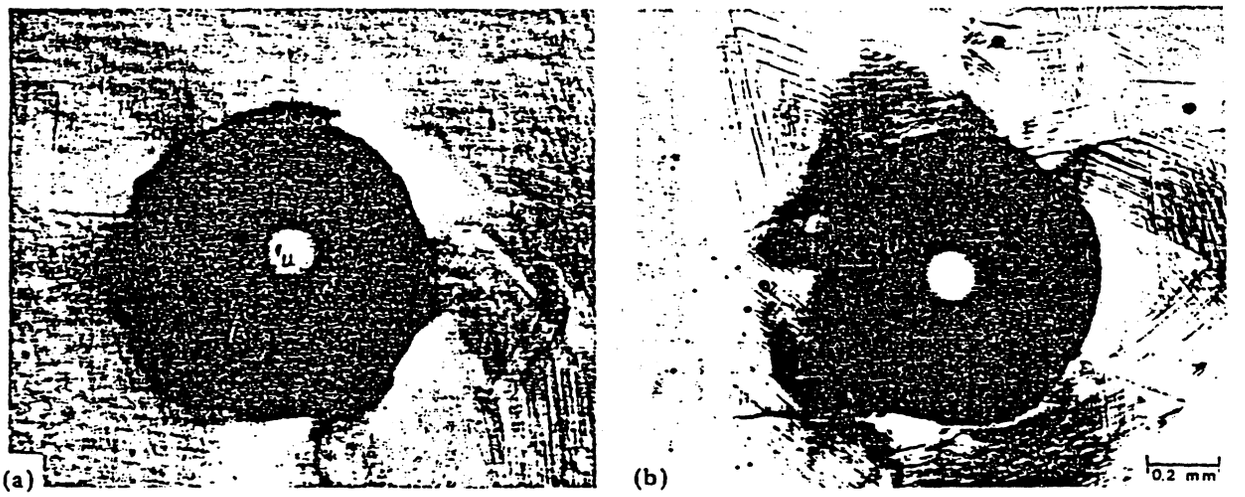


Fig. 5. Spherical indentations in (a) annealed nickel and (b) nickel (preshocked condition) shocked at 25 GPa.

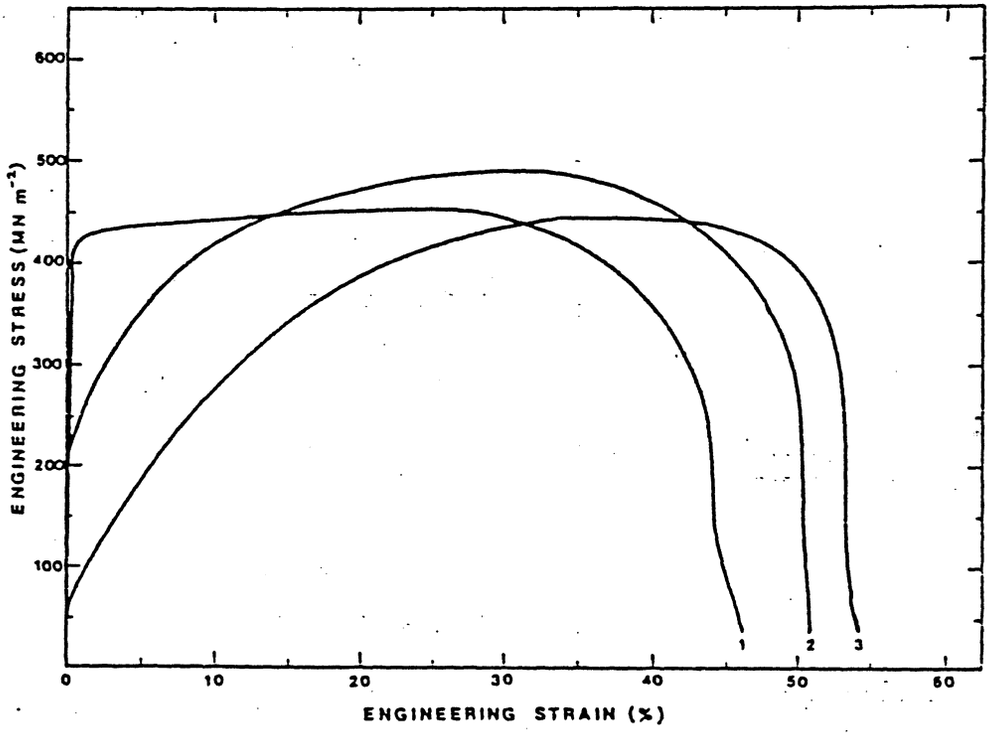


Fig. 6. Tensile response of three metallurgical conditions in the *pre explosionem* state: curve 1, preshocked; curve 2, small grain size; curve 3, large grain size.

position) at four positions within the system: 1.0, 6.5, 13.0 and 19.5 cm from the impact surface. Figure 6 shows the tensile response of the three metallurgical conditions. As expected, the large-grain-size system has the lowest yield stress. Care had to be exercised in the preparation of the specimens; they were machined prior to annealing because the work-hardened surface layer had an unwanted strengthening effect. Figures 7 and 8 show the tensile response in the *post explosionem* condition for the 10 GPa events and 25 GPa events respectively. The decrease in flow stress as a function of distance from the impact surface is consistent with the hardness results and the dislocation substructure [1]. Work softening (*i.e.* a negative work-hardening rate) is only exhibited by the preshocked condition (Figs. 7(c) and 8(c)).

The flow stress and ultimate tensile strength of the specimens taken at 1.0 and 6.5 cm from the top are higher for the small-grain-size

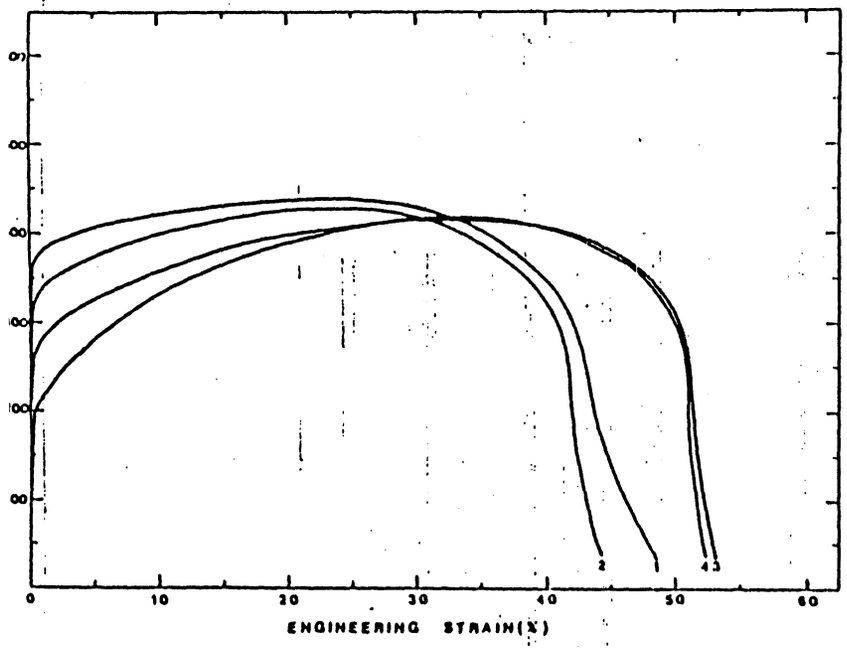


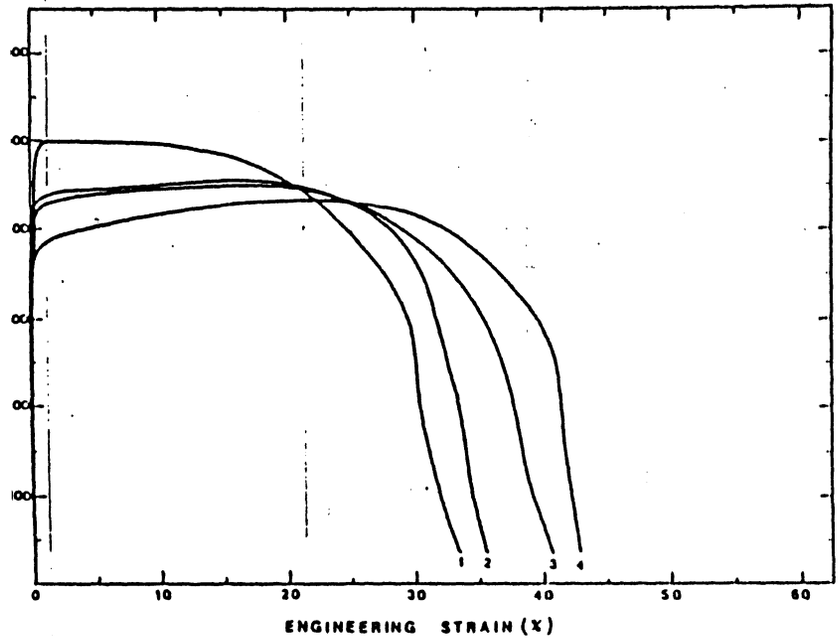


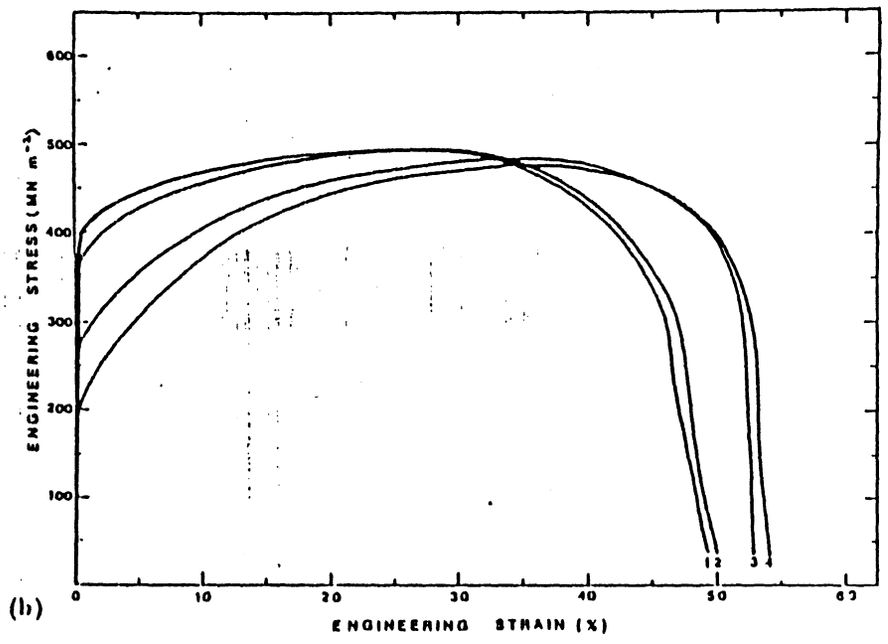


(b)

Fig. 7. Tensile response as a function of distance from the impact interface of the three metallurgical conditions in the *post explosionem* (10 GPa) state: (a) large-grain-size condition; (b) small-grain-size condition; (c) preshocked condition: curves 1, 1.0 cm from the top; curves 2, 6.5 cm from the top; curves 3, 13.0 cm from the top; curves 4, 19.0 cm (a) or 19.5 cm ((b), (c)) from the top.

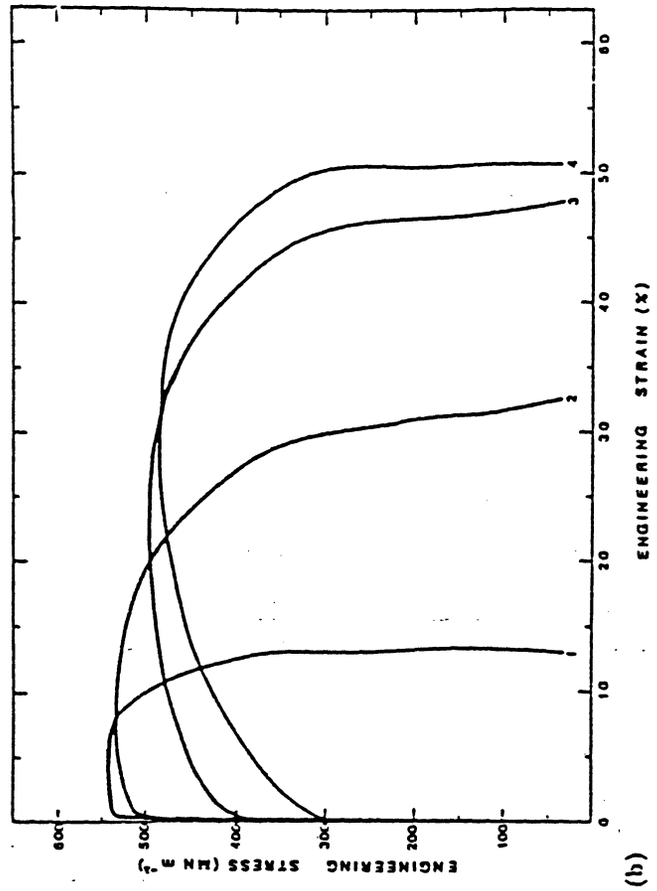


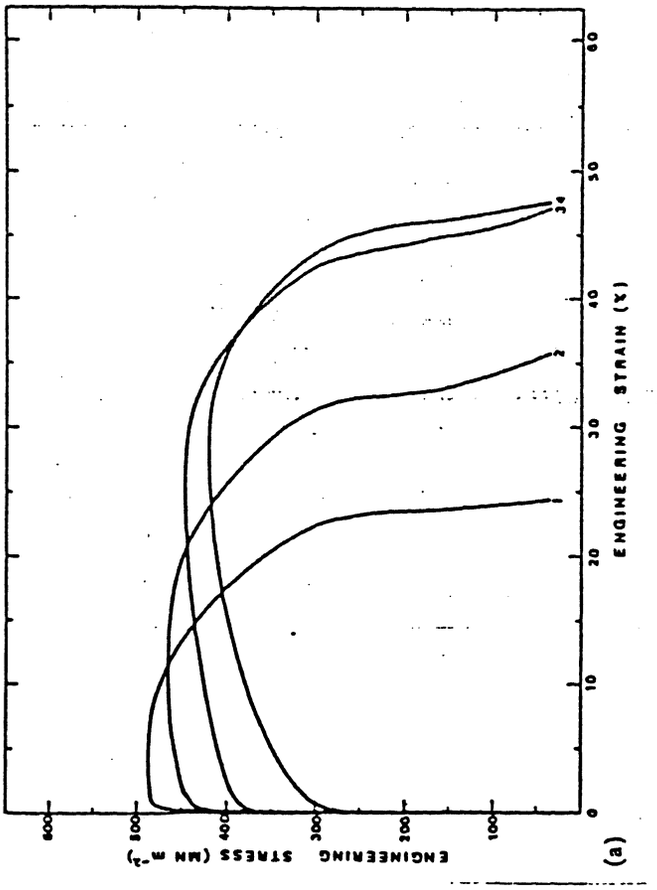


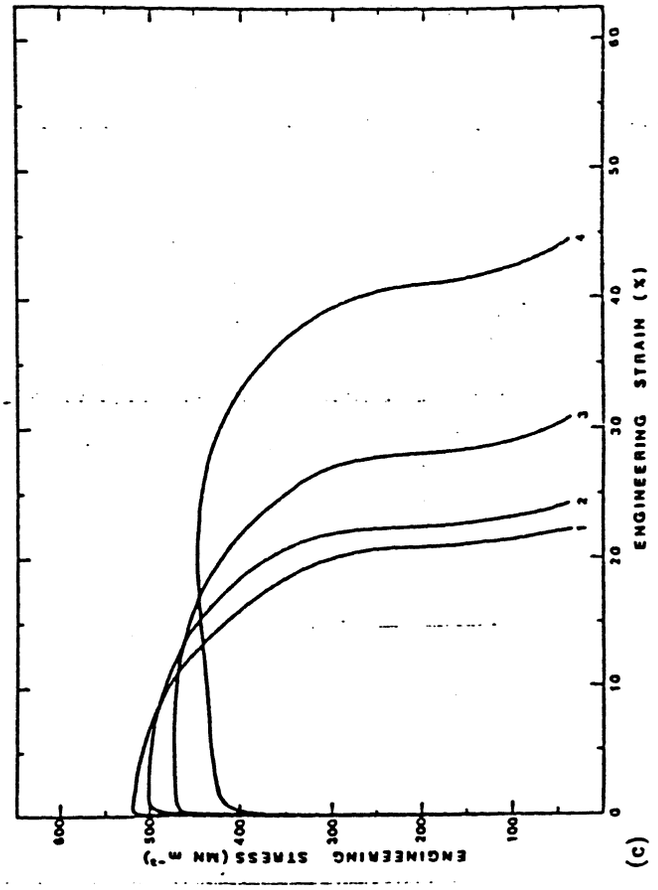


Fig. 8. Tensile response as a function of distance from the impact interface of three metallurgical conditions in the *post explosionem* (25 GPa) state: (a) large-grain-size condition; (b) small-grain-size condition; (c) preshocked condition: curves 1, 1.0 cm from the top; curves 2, 6.5 cm from the top; curves 3, 13.0 cm from the top; curves 4, 19.5 cm from the top.

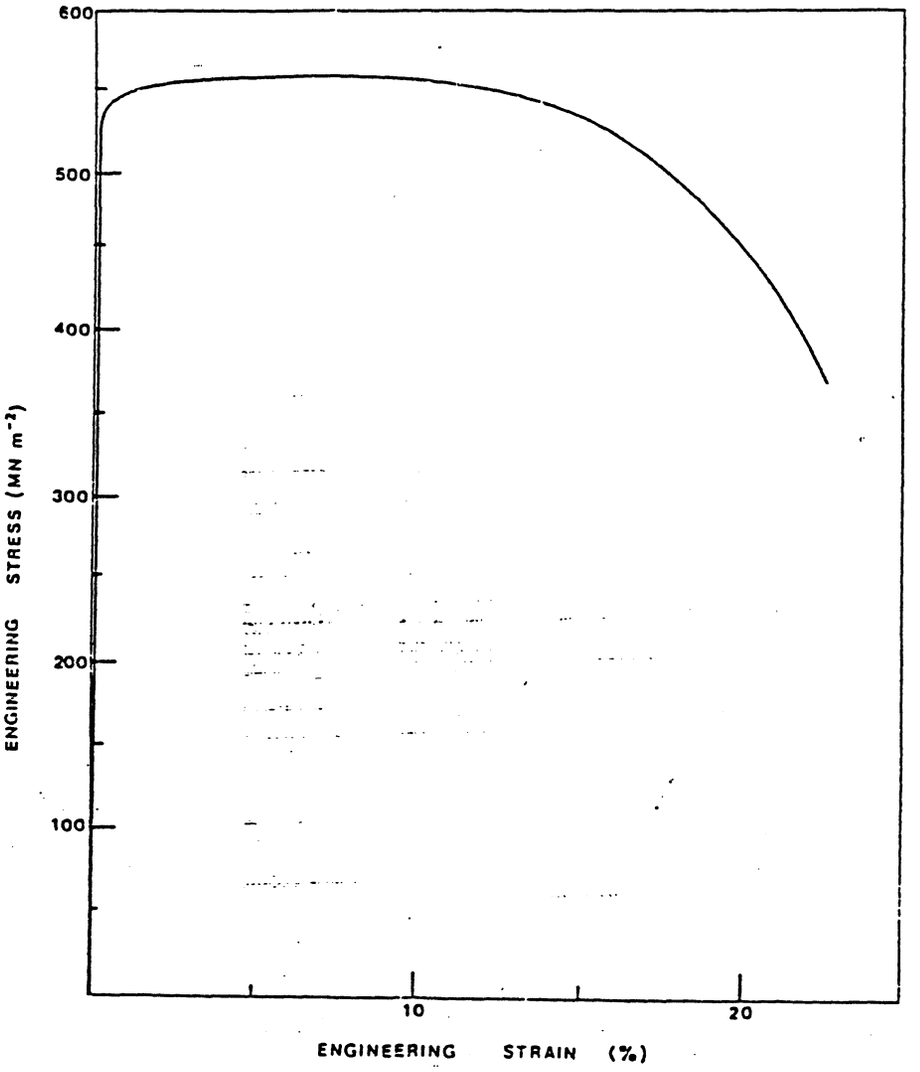


Fig. 9. Engineering stress *vs.* engineering strain curve of nickel cold rolled to a cold-rolling reduction of 20%.

condition at 25 GPa (Fig. 8(b)) than for the preshocked condition at 25 GPa (Fig. 8(c)); these results are consistent with the hardness results. Hence, it can be said that for nickel the grain size effect is greater than the effect of the existing substructure (preshocking) in spite of the fact that, as shown in Fig. 6, the preshocked condition had a higher flow stress.

The substructural instability produced by shock loading and resulting in work softening or a very low work-hardening rate is not nearly as evident after conventional deformation at ambient temperature. Figure 9 shows a specimen cold rolled to a Rockwell A hardness of 58 HRA, higher than that of the preshocked condition shocked at 25 GPa. The flow stress is about 525 MN $m^{-2}$, the same as that of the double-shocked condition in Fig. 8(c). Nevertheless, the cold-rolled specimen clearly exhibits some work hardening, while the double-shocked specimen shows a decrease in stress as soon as the flow stress is reached. Hence, work softening cannot be attributed to "dislocation saturation".

If the hypothesis that the substructure instability is the cause of work softening is correct, then appropriate anneals that stabilize the substructure would eliminate work softening. The annealing response of the various conditions was studied by isochronal treatments (1 h) followed by hardness measurements. As evidenced by Fig. 10, the hardness only starts to decrease after 673 K for the 10 GPa events and after 573 K for the 25 GPa events. The 573 and 673 K annealing treatments for the tensile specimens gave the results shown in Fig. 11. These temperatures were chosen because they did not produce

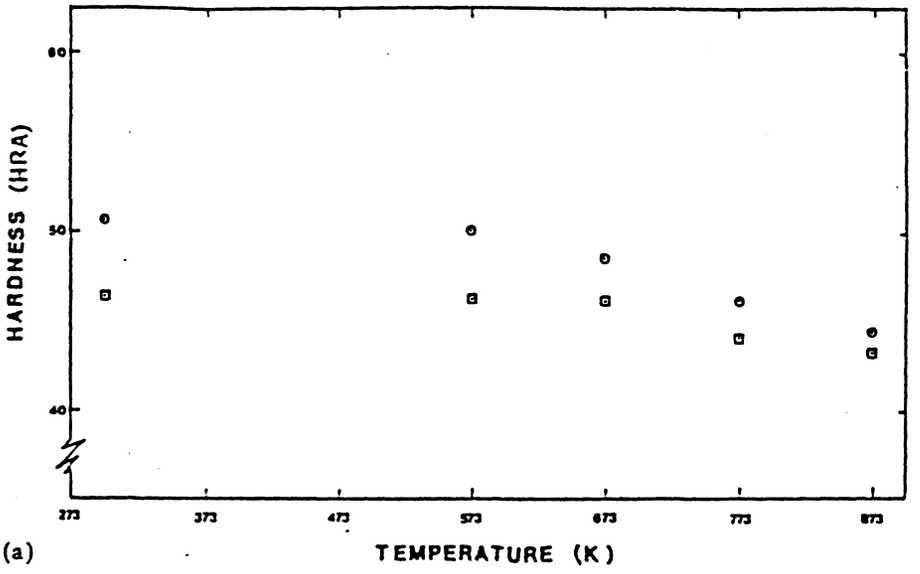


(a)

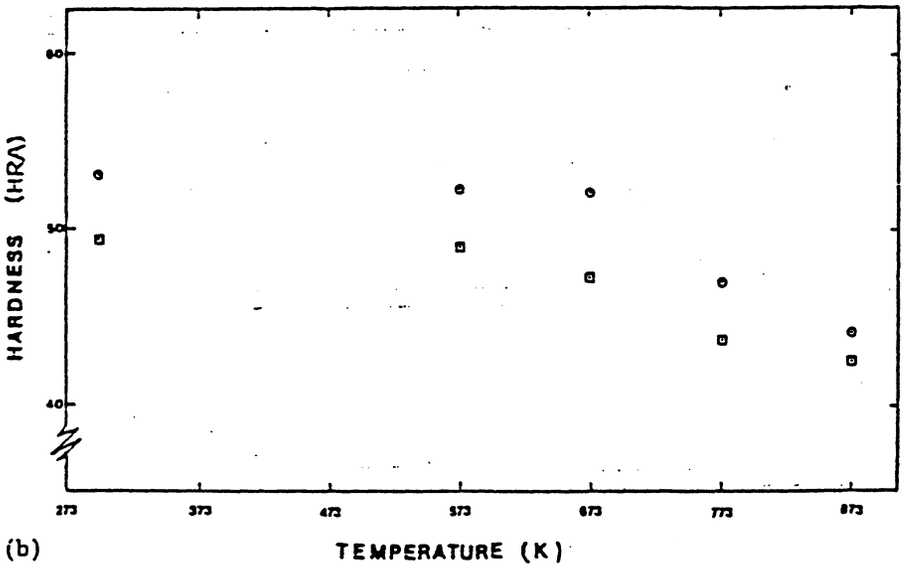


(b)

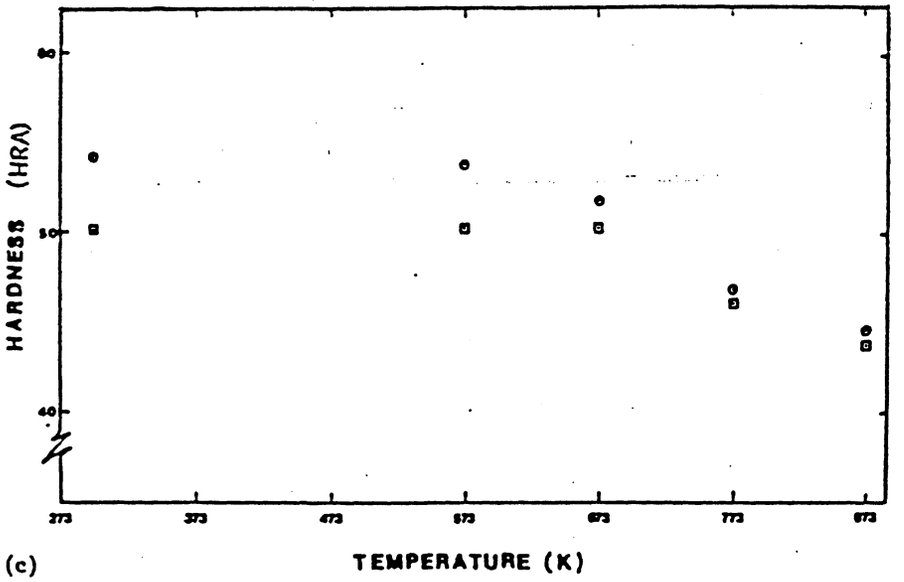


(c)

Fig. 10. Effect of isochronal annealing treatments (1 h) on the hardness of *post explosionem* (a) large-grain-size specimens, (b) small-grain-size specimens and (c) preshocked specimens: ⊙, 25 GPa; ⊡, 10 GPa.

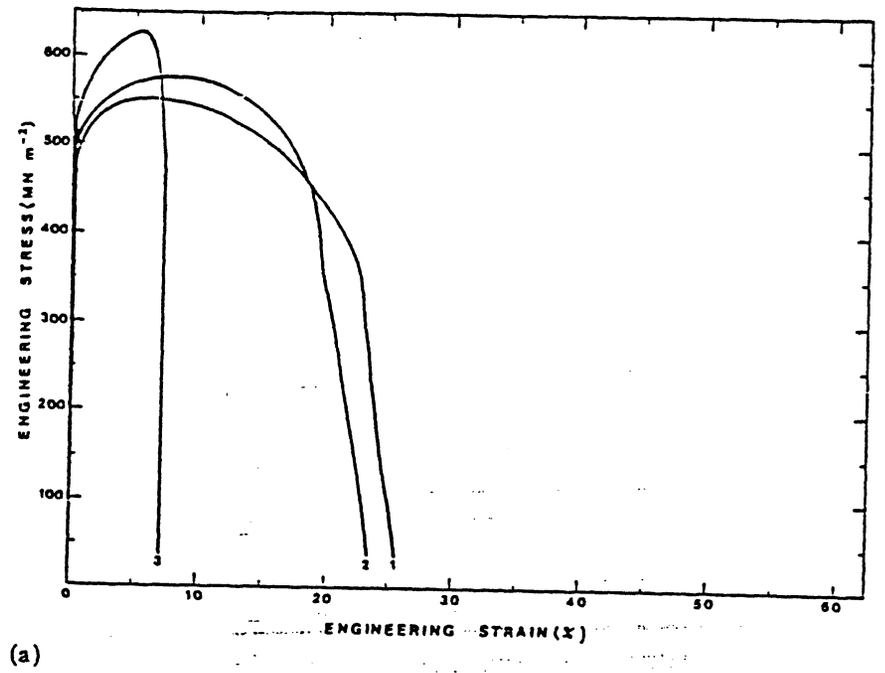


(a)

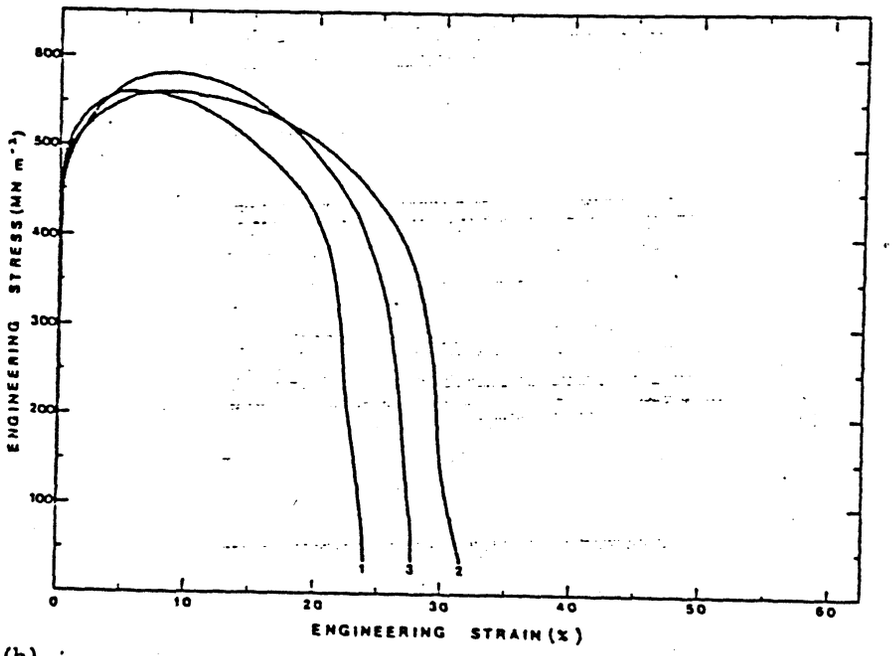


(b)

Fig. 11. Effect of annealing on the tensile response of nickel preshocked and shocked at 25 GPa (specimens taken at a distance of 1 cm from the impact surface); (a) anneal at 573 K for 1 h; (b) anneal at 673 K for 1 h: curves 1, preshocked specimens; curves 2, large-grain-size specimens; curves 3, small-grain-size specimens.

any significant hardness decrease, and recovery (in the classical sense, *i.e.* dislocation annihilation) was kept to a minimum. The tensile curves show clearly how work softening was eliminated, being replaced by work hardening, without a significant decrease in the flow stress (about 500 MN $m^{-2}$). These results confirm that the stabilization of the dislocation substructure eliminates work softening. Willan [22] has previously obtained similar results.

### *3.4. Transmission electron microscopy*

The characterization of the dislocation substructure for the different conditions as a function of distance from the impact—

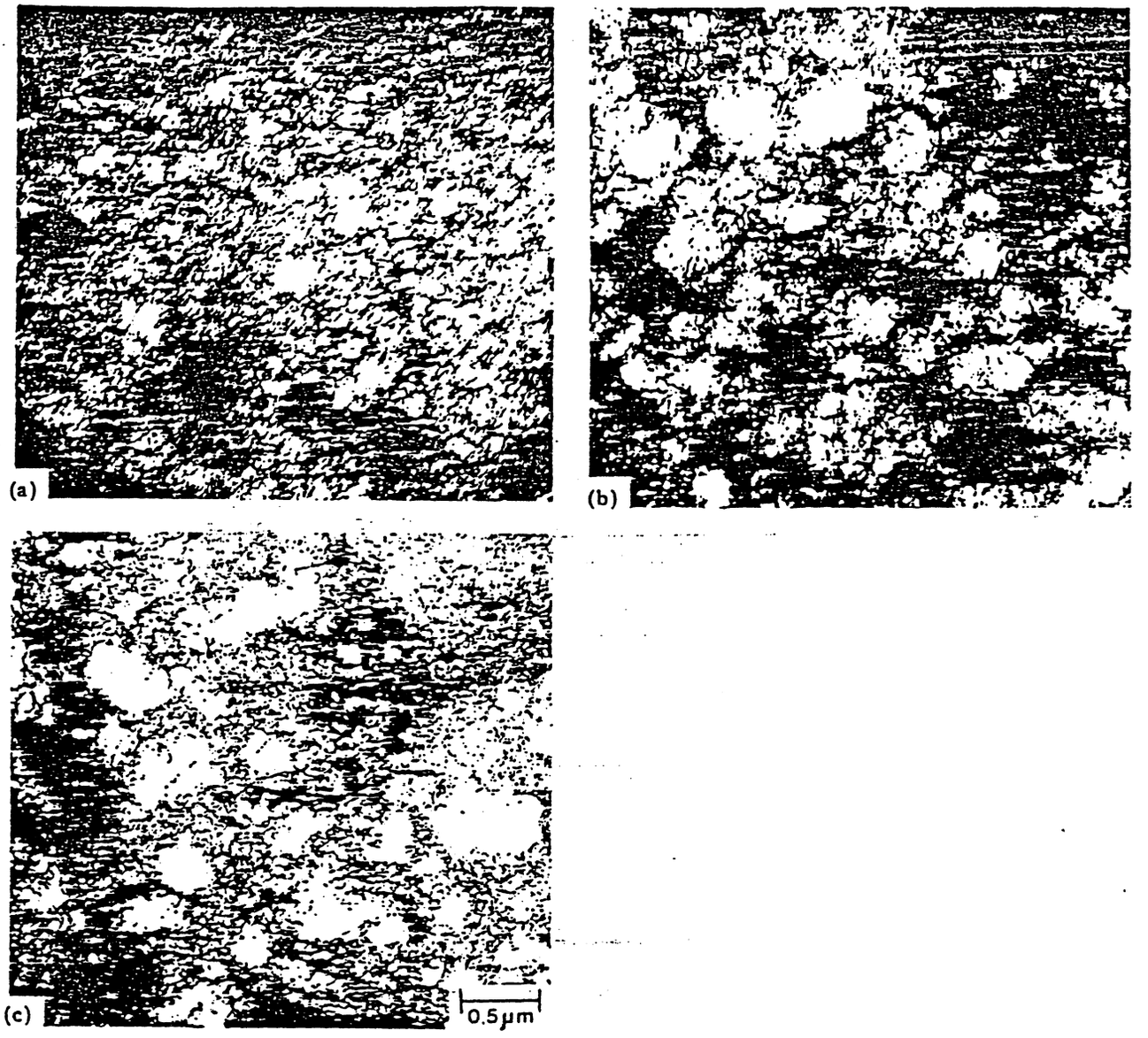


Fig. 12. Transmission electron micrographs showing the effect of annealing on the substructure of nickel (preshocked plus shocked at 25 GPa): (a) double-shocked state; (b) double-shocked state plus anneal at 573 K for 1 h; (c) double-shocked state plus anneal at 673 K for 1 h.

surface has been presented by Hsu *et al.* [1]. The discussion here will be restricted to the annealing and work-softening response. The double-shocked (preshocked plus shocked at 25 GPa) condition exhibits cells with thicker dislocation walls than the singly shocked conditions, in accord with the findings of Kazmi and Murr [23]. Figure 12(a) shows this thick substructure in which cells are not very clearly delineated. Annealing at 573 and 673 K does not produce any dramatic substructural changes; a better definition of the cell interiors and walls is the most obvious change. Figures 12(b) and 12(c) show these changes; a modest decrease in dislocation density with annealing at 673 K can also be seen.

Tensile deformation of the preshocked condition shocked at 25 GPa produced a very significant modification of the dislocation substructure. Foils were removed from the neck region of the tensile specimens and perpendicular to the tensile axis; Fig. 13 shows the formation of bands with high dislocation density; these bands tend to form "islands" as shown in Fig. 13(b). The dislocation density inside the island tends to be lower than that of the original material,

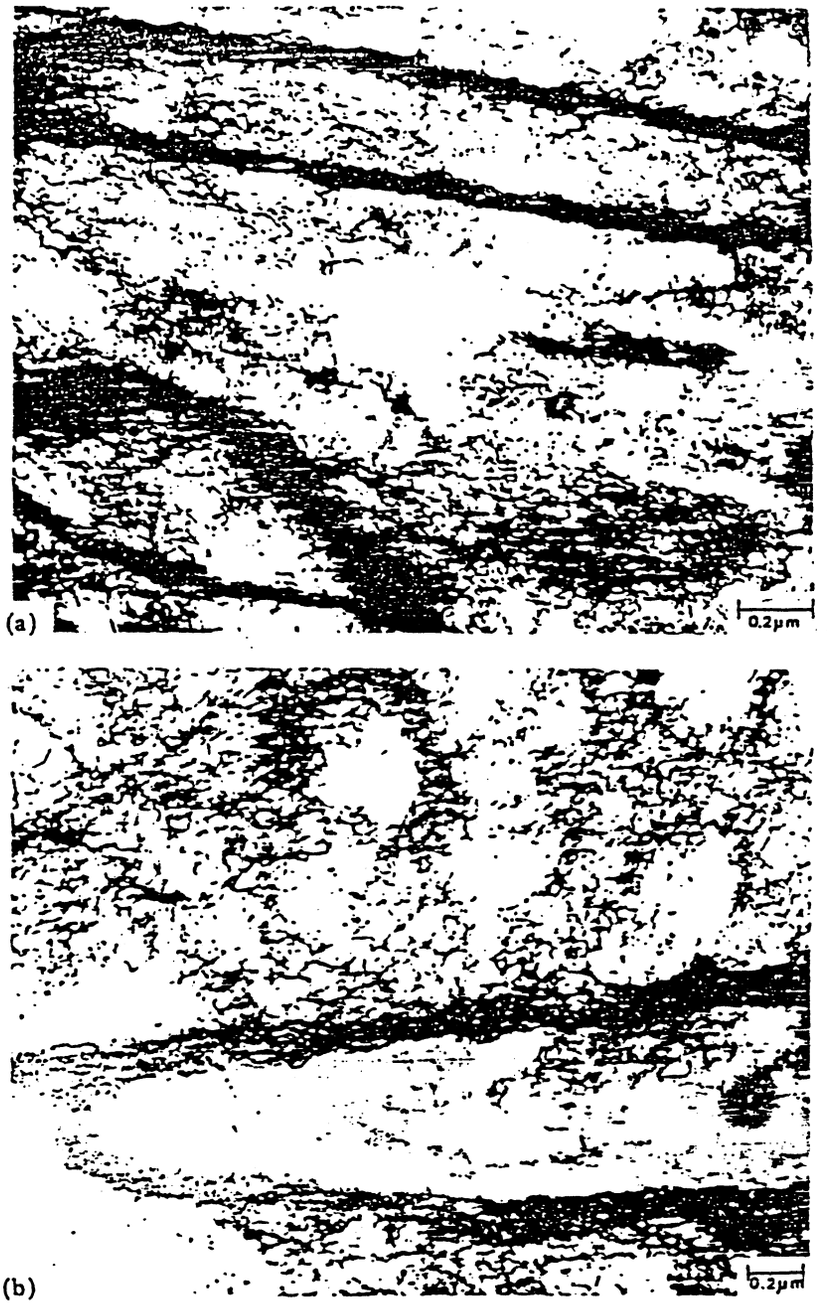


Fig. 13. Two transmission electron micrographs showing the breakdown of shock-wave-induced substructure occurring at the neck region of a tensile specimen (the effect of work softening).

indicating that the dislocations leave the original equiaxed cells to form the elongated islands, during tensile deformation. The walls of these islands have a very high dislocation density, as evidenced by the complete extinction in Figs. 13(a) and 13(b). The misorientation produced by the cell wall in Fig. 13(b) was found by the asterism in the diffraction pattern; it is equal to approximately 3°.

A mechanistic interpretation of the processes involved in the formation of these islands transcends the scope of this paper. Nevertheless, a few qualitative comments can be advanced. The shock-induced dislocation substructure should have a net Burgers vector equal to zero, since the residual strain is zero, under ideal uniaxial strain conditions. Indeed, Meyers [24] has proposed a model according to which adjacent layers of dislocations with opposite Burgers vectors are homogeneously generated as the shock front propagates through the metal. These dislocations would organize themselves into low energy configurations forming dipolar walls [25]. These


Fig. 14. Elongated dislocation cells observed in a specimen cold rolled to a 20% reduction in thickness; the similarity with the cells shown in Fig. 13 should be noted.

dipolar walls are distinct from cell walls, which are small-angle boundaries; the dipolar walls are "assemblies of dislocations, primary in edge orientation, mostly belonging to the same glide system, spread out normal to the glide direction, and with roughly equal frequency of positive and negative Burgers' vector direction" [26]. The recent paper by Fourie *et al.* [26] provides a comprehensive classification scheme for dislocation arrays; the collective behavior of dislocation arrays, whose study has been pioneered by Kuhlmann-Wilsdorf, is still not well understood at the present time. Charsley and Kuhlmann-Wilsdorf [27] have recently investigated dislocation walls in a Cu–Ni alloy; they found that the dipolar walls forming at right angles would not intersect themselves or terminate in the matrix, thereby forming arrangements that would resemble the cellular tangled arrays typical of shock loading. Kuhlmann-Wilsdorf [25] predicts that the effect of glide (by tensile extension at a slow strain rate) on these dipolar walls forming a pseudocell structure would be disruptive, because the energy of these arrays is high and their configuration would be unstable. Therefore, glide would tend to continue where it first began, resulting in work softening.

Figure 14 shows a similar type of elongated cell after cold rolling to a reduction of 20%. Clearly, this type of substructure is characteristic of deformation at slow strain rates (extension in tensile testing and cold rolling are fairly similar). Hence, the rationale provided by Longo and Reed-Hill [14–16] is confirmed. The dislocation substructure produced by shock loading is transformed, by further straining during tensile testing, into the dislocation substructure stable under the imposed conditions (the substructure shown in Fig. 14). The hypothesis that dislocation climb is responsible for work softening can be safely discarded by a simple calculation. On the assumptions of a dislocation density of $10^{10}$ cm$^{-2}$ and a point defect concentration of $7 \times 10^{-5}$ and that all the point defects diffuse towards the dislocations, a climb of one atomic position would be obtained. This is, obviously, not sufficient to alter in any significant way the deformation path of the dislocations.

## 4. CONCLUSIONS

(a) The attenuation of shock waves in nickel was found to be independent of the initial metallurgical condition; the metallurgical variables were the grain size and *pre*

*explosioncm* dislocation substructure. The attenuation rate exceeds substantially that predicted from hydrodynamic theory.

(b) The decrease in shock-induced dislocation density as a function of distance from the impact surface is consistent with the decrease in hardness and modification of the tensile response.

(c) On ambient temperature tensile testing, work softening was observed for the specimens in the preshocked condition and for the specimens shocked at 25 GPa. Work softening was eliminated by an appropriate anneal that stabilized the substructure without significantly affecting the yield stress.

(d) Transmission electron microscopy observation of the neck region that underwent work softening revealed that the substructure characteristic of shock loading (a high dislocation density in cellular arrays with ill-defined walls) was replaced by elongated cells with very well-defined walls. The latter substructure is apparently more stable under the imposed conditions. It is suggested that the dislocation arrays generated in shock loading are dipolar walls; the pseudocell structure formed has a high energy configuration which is unstable if glide is initiated in a plane.

## ACKNOWLEDGMENTS

This research program was supported by National Science Foundation Grants DMR-7927102 and DMR-8115127. The help of Mr. P. S. de Carli, Stanford Research Institute, in the execution of the explosive events is gratefully acknowledged. Special gratitude is extended to Professor L. E. Murr, Oregon Graduate Center, for help with the transmission electron microscopy and the valuable input through discussions and to Professor D. Kuhlmann-Wilsdorf, University of Virginia, for helpful clarification of the nature of dislocation arrays and of the interpretation of the changes undergone by the shock-induced dislocation substructures.

## REFERENCES

1 C. Y. Hsu, K.-C. Hsu, M. A. Meyers and L. E. Murr, in M. A. Meyers and L. E. Murr (eds.), *Shock Waves and High-strain-rate Phenomena in Metals: Concepts and Applications*, Plenum, New York, 1981, p. 433.
2 M. A. Meyers, L. E. Murr, C. Y. Hsu and G. A. Stone, *Mater. Sci. Eng., 57* (1983) 113.
3 Lord Raleigh, *Proc. R. Soc. London, Ser. A, 84* (1910) 247.
4 G. I. Taylor, *Proc. R. Soc. London, Ser. A, 84* (1910) 371.
5 J. von Neumann and R. D. Richtmyer, *J. Appl. Phys., 21* (1949) 232.
6 J. O. Erkman, *Phys. Fluids, 1* (1958) 535.
7 W. E. Drummond, *J. Appl. Phys., 28* (1957) 1437.
8 G. R. Fowles, *J. Appl. Phys., 31* (1960) 655.
9 J. R. Rempel, D. N. Schmidt, J. O. Erkman and W. M. Isbell, *SRI Tech. Rep. WL-TR-65-119*. 1965 (Stanford Research Institute) (U.S. Air Force Weapons Laboratory Contract AF 29(601)-6040).
10 J. O. Erkman, A. B. Christensen and G. R. Fowles, *SRI Tech. Rep. AFWL-TR-66-12*, 1965 (Stanford Research Laboratory) (U.S. Air Force Weapons Laboratory Contract AF 29(601)-6734).
11 J. O. Erkman and A. B. Christensen, *J. Appl. Phys., 38* (1967) 5395.
12 D. R. Curran, *J. Appl. Phys., 34* (1963) 2677.
13 M. A. Meyers, *Metall. Trans. A, 8* (1977) 1581.
14 W. P. Longo and R. E. Reed-Hill, *Scr. Metall., 4* (1970) 765.
15 W. P. Longo and R. E. Reed-Hill, *Scr. Metall., 6* (1972) 833.
16 W. P. Longo and R. E. Reed-Hill, *Metallography, 7* (1974) 181.
17 C. Y. Hsu, *M.Sc. Thesis*, New Mexico Institute of Mining and Technology, Socorro, NM, 1980.
18 K.-C. Hsu, *M.Sc. Thesis*, New Mexico Institute of Mining and Technology, Socorro, NM, 1981.
19 M. A. Meyers and L. E. Murr (eds.), *Shock Waves and High-strain-rate Phenomena in Metals: Concepts and Applications*, Plenum, New York, 1981, Appendix F, p. 1059.
20 B. Tabor, *The Hardness of Metals*, Clarendon, Oxford, 1951, p. 15.
21 R. Böklen, in J. H. Westbrook and H. Conrad (eds.), *The Science of Hardness Testing and its Research Applications*, American Society for Metals, Metals Park, OH, 1973, p. 109.
22 W. C. Willan, Jr., *M.Sc. Thesis*, South Dakota School of Mines and Technology, Rapid City, SD, 1977.
23 B. Kazmi and L. E. Murr, cited in M. A. Meyers and L. E. Murr (eds.), *Shock Waves and High-strain-rate Phenomena in Metals: Concepts and Applications*, Plenum, New York, 1981, p. 733.
24 M. A. Meyers, *Scr. Metall., 12* (1978) 21.
25 D. Kuhlmann-Wilsdorf, University of Virginia, personal communication, 1982.
26 J. T. Fourie, P. J. Jackson, D. Kuhlmann-Wilsdorf, D. A. Rigney, J. H. van der Merwe and H. G. F. Wilsdorf, *Scr. Metall., 16* (1982) 157.
27 P. Charsley and D. Kuhlmann-Wilsdorf, *Philos. Mag., 44* (1981) 1351.